An Investigation on the Influence of Nickel Contamination on Thermal Fatigue Reliability of Jumper Pins Plated Through Hole (PTH) Solder Joints

David Hillman, Tim Pearson, Ross Wilcoxon, Parker Jacobson
Collins Aerospace

Denis Jean
MacDermid Alpha Electronic Solutions

ABSTRACT

An investigation was conducted to examine the validity of current industry maximum nickel contamination limits, which are established to ensure plated through hole solder joint integrity, for SnPb and SAC305 solder baths. A reassessment of these limits is necessary because current industry specifications allow for little, or even zero, element contamination above what is allowed in virgin solder material, which is not practical in a manufacturing environment. Moreover, most work that has been done to assess the impact of nickel contamination on lead-free solders has focused on its impact on processing parameters rather than the reliability of resulting solder joints. For this investigation, test vehicles were processed using three levels of nickel contamination for each solder: 0.01 wt.%, 0.02 wt.%, 0.05 wt.% for SnPb solder and 0.05 wt.%, 0.07 wt. %, 0.10 wt.% for SAC305 solder. The test vehicles were subjected to thermal cycle testing in accordance with the IPC-9701 specification. After more than 7500 thermal cycles, there were insufficient failures to characterize the failure distributions of the solder joints for any of the test combinations. Assessment of early failures did not find a correlation between higher nickel content, within the ranges investigated, on solder joint integrity. Therefore, the authors recommend that the allowable nickel contamination levels listed in the IPC-J-STD-001 specification (Table 3-1, Maximum Limits of Solder Bath Contaminant) be 0.05 wt.% for SnPb Assembly, 0.05 wt.% for SnPb Preconditioning, and 0.10 wt.% for SAC305 Pb-free Assembly.

Key words: nickel contamination limits, plated through hole soldering

INTRODUCTION

The functional characteristics and physical properties of metallic alloys are heavily dependent on their constituent elemental compositions. For the electronics industry, solder alloy compositions and the allowable solder alloy contaminants are defined in IPC-J-STD-006, Requirements for Electronic Grade Solder Alloys. This specification also establishes allowable element contamination limits, as determined by industry and solder alloy supplier investigations conducted in the 1960's through 1970's. One such contaminant element is nickel. Historically, selective solder and wave solder processes introduce limited nickel contamination when they are used with circuit board surface finishes such as Hot Air Solder Level (HASL) or Fused SnPb plating. The IPC-J-STD-001 specification requires periodic testing for solder alloy contamination for production solder baths. When processing HASL or Fused SnPb surface finishes, it is rare that the maximum nickel contamination limits are exceeded. However, the growing use of Electroless Nickel/Immersion Gold (ENIG) printed circuit board surface finish and nickel-containing component surface finishes have increased the likelihood that solder baths will exceed their maximum nickel contamination limits.

The impact of elemental impurities on SnPb solder alloy properties was established by Heberlein in 1962 [1]. Heberlein's investigation focused on the wettability, adhesion and corrosion aspects of SnPb solder for protective coating of low carbon steel, copper and brass sheets. The impacts of arsenic, antimony, sulfur, phosphorus, copper, silver and bismuth were qualitatively evaluated. Bismuth and silver were found to have no harmful effects for the values tested. For the remaining elements, proposed element maximum contamination levels recommendations were made to the ASTM B32 committee.

In the late 1970s and 1980s, significant efforts on solder impurities were conducted by the International Tin Research Institute (Ackroyd at al [2], MacKay [3-5]) and the Swedish Institute for Metals Research (Steen and Becker [6]). These investigations were in response to a lack of industry data, national specification consistency (i.e., US Military QQ-S-571, ASTM B32, German DIN1707, British BS219) and the rapid implementation of mass soldering processes. Their research focused on the Sn60Pb40 solder alloy for a variety of elements and elemental impurity levels. They characterized the influence of elemental contamination on oxidation behavior, solidification behavior, surface energy, wetting forces and solder spread characteristics. The investigations used a range of flux formulations and base metals including copper, brass and steel. Measurements gathered using wetting balance were statistically analyzed and used to establish solder alloy element impurity recommendations that addressed two factors: 1) solder alloy element impurity level values for the national standards that result in acceptable, ideally defect-free solder joints; 2) solder alloy maximum element contamination levels that provide acceptable margins between virgin solder alloy ingots and mass solder process baths. Over a period of several years, the electronics industry solder suppliers and national specification committees used these recommendations to evolve the element contamination levels found in the IPC-J-STD-001 and the IPC-J-STD-006 specifications used for modern soldering processes. These elemental contamination limits have been given a periodic cursory examination (Bernier [7]), but few changes have been made.

The introduction of Pb-free solder alloys and soldering processes, due to the implementation of the Restriction of Hazardous Substances (RoHS) environmental legislation, has renewed interest in solder alloy metallurgy. This has led to new research on, for example, element dissolution (Hillman et al. [8]), constituent elemental solder alloy additions (Wu and Wong [9]) and solder joint durability (Coyle et al. [10]). However, there have been limited investigations on the effects of elemental contamination levels for Pb-free solder alloys with the same diligence was as that used with SnPb solder alloys. Gickler et al. [10] examined the impact of copper and lead on the solder joint microstructure of several Pb-free alloys but did not characterize the solder alloy properties. Forsten et al. [11] investigated the interaction of Pb-free solder and the wave soldering process in terms of equipment compatibility. That study provided excellent data on the wave soldering process control aspects of copper and nickel dissolution, but no solder joint reliability data were generated. Diepstraten and Trip [13] studied the effectiveness of using the IPC-J-STD-001 specification limits for assessing the result of wave solder contamination on the SAC305 solder alloy. The impact of lead, copper, nickel, phosphorus and silver on solder joint microstructure, wave solder process control limits and wetting/fluidity were measured. Nogita et al. [15] and Ramli et al. [16] conducted extensive studies on the influence of nickel and bismuth on the solder wetting, surface energy, solder microstructure and intermetallic compounds formation of the Sn-0.7Cu solder alloy. Again, these studies produced valuable information, but no solder joint reliability data were generated. The IPC Solder Products Value Council (SPVC) completed an investigation of the SAC305 solder alloy "take action limits" for solder baths/pots as they identified inconsistent element compositional maximum limits from their membership [17]. The investigation focused on a wide range of maximum element additions using wetting balance testing protocols. The wetting time/force were measured and metallurgical cross-sectional analysis was completed for bulk alloy/intermetallic phase characterization. The investigation did not identify any significant impact of contamination on the measured solder alloy properties and the IPC SPVC recommended maximum element levels "at which the solder pot should be adjusted to ensure reliable solder performance of the solder joint". However, the study did not include any solder joint durability testing to validate the proposed maximum element values.

In the long history of research on the influence of element impurities and maximum allowable levels in solder baths/pots, there is a fundamental difference between the goals of the early SnPb alloy research and those of more recent Pb-free alloy investigations. The objective of the SnPb alloy research was to define impurity limits that ensured acceptable solder joints for the national specifications. The ultimate solder joint durability of the resulting SnPb solder compositions was the responsibility of the design community. Segments of the Pb-free alloy research had the same objective but as demonstrated by the IPC SPVC study, many of the investigation/studies did not include solder joint reliability testing in their plans. The lack of reliability testing is not surprising given the proliferation of Pb-free solder alloys and the cost associated with conducting solder joint durability testing. This has led to maximum allowed element impurity levels, per the IPC-J-STD-006 virgin solder bar specification, that are very close to the allowable impurity assembly process limits, per the IPC-J-STD-001 specification. The SnPb maximum nickel impurity level is the most problematic assembly issue as the virgin bar limit of 0.01 weight % maximum is identical to the assembly process limit of 0.01 wt. % maximum. Thus, acceptable virgin solder could potentially begin at the maximum allowable limit such that any a small amount of additional nickel contamination occurring during use would cause the solder bath to be out of specification.

Therefore, the objective of the investigation was to examine the validity of current industry specification maximum nickel contamination limits for SnPb and SAC305 solder baths by evaluating their impact on plated through hole solder joint integrity.

PROCEDURE

Test Vehicle

The test vehicle used for the investigation was fabricated in accordance with IPC-6012, Class 3, Type 4. Each test vehicle was 4.6 inches x 4.2 inches x 0.068 inches and included 8 copper layers. The test boards were procured with two surface different finishes: electroless nickel/immersion gold (ENIG) surface finish in accordance with IPC-4552 and immersion silver (ImAg) in accordance with IPC-4553. Each test vehicle contained 24 daisy chained pairs and 12 pairs of non-daisy chained pairs of 0.082 inch +/- 0.003-inch diameter plated through holes. Only the 24 pairs of daisy chained plated through holes were used in the investigation. A total of 120 test vehicles were processed for each parameter set (nickel contamination level/solder alloy composition) in the investigation. Figure 1 illustrates the test vehicle.

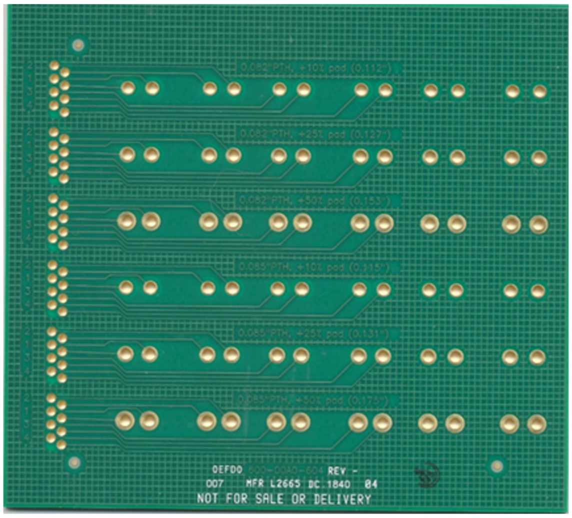

Figure 1. Investigation Test Vehicle

Test Components

The test components were Mill-Max shorting jumpers to simulate plated through hole components and enable the use of event detector electrical resistance monitoring equipment. The primary shorting jumper had a surface finish of 10 microinch gold over nickel (Au/Ni) underplating on a brass pin, representing a nickel contribution worst case. A small number of shorting jumpers had a surface finish of 200-300 microinch tin plating over nickel (Sn/Ni) underplating on a brass pin, which allowed for the inclusion of a potential "tin whisker observed variable" in the investigation. Figure 2 illustrates the shorting jumpers used.

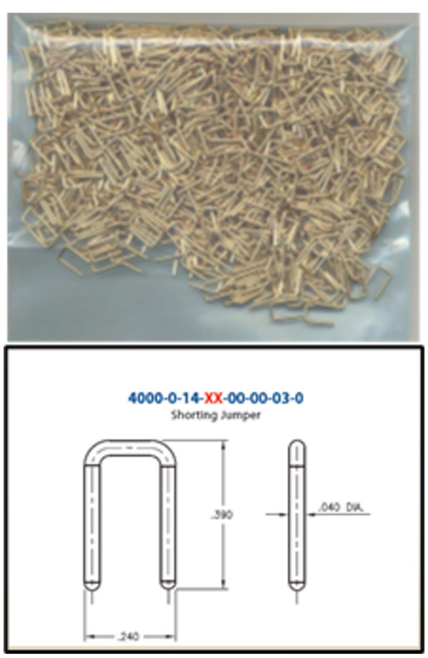

Figure 2. Investigation Test Components (Top: As Received Parts, Bottom: Jumper Dimensions)

Solder Alloys

Two solder alloys were included in the investigation: Sn63Pb37 (SnPb) and SAC305 (Pb-free). These two alloys are the primary solder alloys used on Collins Aerospace products and in the Aerospace/Defense industry electronics sector. Three different solder bath nickel contamination levels were used for each solder alloy to characterize the impact on solder joint integrity for each solder alloy (Table 1). These nickel contamination levels included the current IPC-J-STD-001 maximum specification limit and two higher nickel content levels. Because Collins Aerospace does not have the capability to produce solder alloys with different nickel contamination levels, Collins collaborated with MacDermid Alpha Electronic Solutions, which produced the contaminated solder alloys in billet form.

Table 1. Investigation Solder Alloy and Nickel Contamination Levels

Solder Alloy	Baseline Level	Level 1	Level 2
SnPb	0.01 wt.%	0.02 wt.%	0.05 wt.%
SAC305	0.05 wt.%	0.07 wt.%	0.1 wt.%

Assembly

The test vehicles were assembled using an AirVac PCBRM12 mini-wave soldering system with an AirVac FW12-88 nozzle. A solder alloy at a prescribed nickel contamination level was loaded into the soldering system and thoroughly circulated for 15 minutes prior to the soldering process to ensure a uniform solder pot metallurgy. The plated through holes were manually pre-fluxed using Alpha UP78 paste flux. Minor solder drossing of the test vehicle soldermask did occur, but it was easily removed with careful light brushing. After each set of test vehicles was assembled, samples of solder were removed from the bath for metallurgical analysis prior to the removal of the solder alloy from the solder pot. The mini-wave solder pot was emptied and "flushed" using pure tin solder bar between each occurrence of the solder alloy test vehicle assembly processing.

Each of the test vehicles were placed in an Electrovert Aquastorm 200 in-line cleaning system for removal of solder flux residues. The in-line cleaner utilized Kyzen Aquanox 4625 saponifier in deionized water. One set of test vehicles was subjected to metallographic cross-sectional analysis without being exposed to thermal cycling to serve as "time zero" samples to validate that adequate solder fill/wetting was achieved. Figure 3 illustrates one of the typical "time zero" plated through hole solder joints.

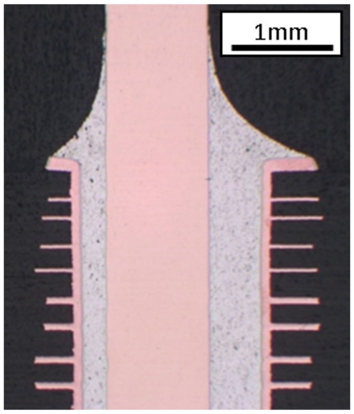

Figure 3. Cross-section of "Time Zero" SnPb Soldered Shorting Jumper Confirming Solder Fill and Wetting

Thermal Cycling

The test vehicles were placed in a thermal chamber set for a temperature range of -55°C to 125°C. The ramp rate was set for 5°C - 10°C per minute and a minimum 10-minute dwell at each temperature extreme. A total of 1688 individual solder joints were wired for continuously monitoring continuity throughout thermal cycle testing with the event detector, in accordance with the IPC-9701 specification. An "event" was recorded if the resistance of a channel exceeded 300 Ω for longer than 0.2 µsec within a 30 second period.

A failure was defined as a component that met one or more of the following conditions:

- Exceeded the maximum resistance for 15 consecutive events; or
- Had five consecutive detection events and proceeded to record at least 15 events; or
- Became electrically open

Figure 4 illustrates the test vehicle "brick" prepared for testing while Figure 5 shows the thermal cycle temperature profiles measured on multiple test boards. A total of 7,581 thermal cycles were completed.

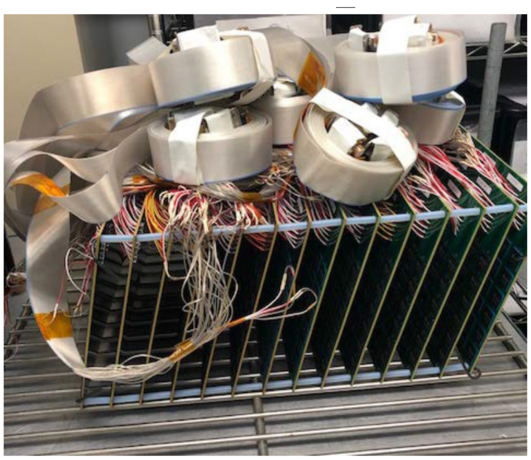

Figure 4. Test Vehicle "Brick" for Thermal Cycle Testing

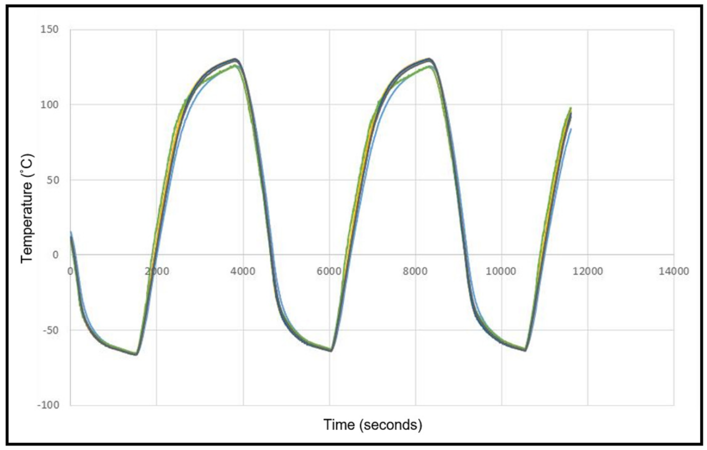

Figure 5. Thermal Profile

RESULTS

Statistical Analysis

The solder joint thermal cycle integrity data was analyzed using regression analysis to determine the Weibull shape factor (β) and characteristic life (θ). The Weibull function relates the cumulative failure distribution, F(n), to the number of thermal cycles at which a failure occurred, n, as:

$$F(n) = 1 - \exp\left(-\frac{n}{\theta}\right)^{\beta}$$

The characteristic life in a Weibull distribution, θ, corresponds to the number of cycles at which 63.2% of the population is expected to have failed. This parameter is often referred to as "N63" and may be thought of as an indication of the approximate average life of the population. The shape factor (β) is often referred to as the Weibull slope and is a measure of how tightly grouped the failures are. The lower the shape factor, the wider the range of failure data (i.e., a wider range of thermal cycles where failures are seen). The higher the shape factor, the more uniform the reliability across the population is; if all components fail at exactly the same point the shape factor would be infinity. A shape factor of less than 1.0 is generally considered to be indicative of infant mortality. Electronic components in thermal cycling that are undergoing 'post infant mortality' failures have typically exhibited shape factors in the range of 4-8, depending on the particular packaging style.

Figure 6 shows cumulative failure distributions for test components plated with Au/Ni and assembled with SnPb solder with three levels of Ni contamination (0.01, 0.02, and 0.05%). This plot shows measured failure data (symbols) for both board surface finishes (ENIG and ImAg) and includes lines that indicate the calculated Weibull distribution for each data set. The plot does not indicate any consistent trends between the level of nickel contamination and the populations' failure characteristics. More importantly, the data show that only a very small portion of the population failed by the end of testing. The highest measured failure rate, which was seen on components assembled to ImAg boards with solder that had

0.02% contamination, was less than 12%. In general, a population should experience at least ~25% failures in order to generate a reasonable estimate of its Weibull distribution coefficients.

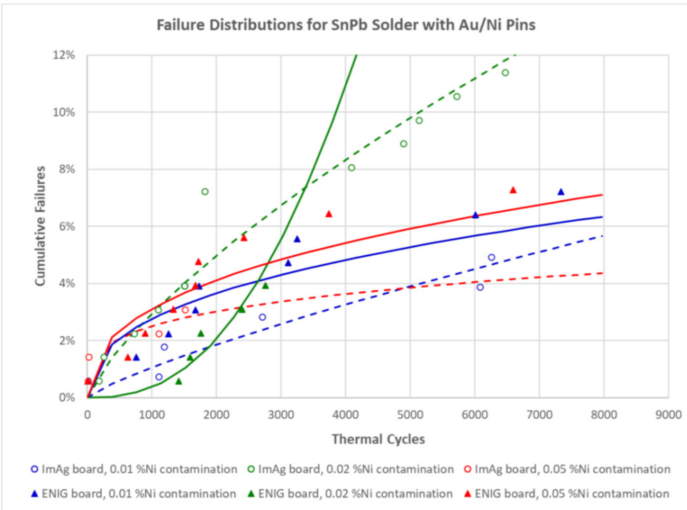

Figure 6. Cumulative Failure Distributions for SnPb Solder and Au/Ni Plated Pins

Table 2, Table 3, and Table 4 show statistical results for ImAg and ENIG boards with each contamination level tested for a given combination of solder (SnPb or SAC305) and pin metallization (Au/Ni or Sn/Ni). For combinations with at least three failures, Weibull coefficients are shown; however, given the low failure rates seen at the end of testing these values have substantial uncertainty. In nearly every case, the calculated value of the Weibull slope (beta) is less than 1, which indicates that the recorded failures are likely associated with infant mortality.

Table 2. Statistics for SnPb Solder with Au/Ni Pin Plating

SnPb Solder with Au/Ni Pins							
Board Type		ImAg			ENIG		
%Ni Contamination		0.01	0.02	0.05	0.01	0.02	0.05
Population statistics	# failed	5	14	4	9	5	9
	# did not fail	90	106	116	111	114	110
	# samples	95	120	120	120	119	119
Failure statistics	rate	5.3%	11.7%	3.3%	7.5%	4.2%	7.6%
	first	1108	178	16	12	1411	9
	average	3466	2600	667.5	2791	1983	2111
	median	2707	1503	569	1732	1760	1677
	last	6253	6469	1516	7330	2753	6589
Weibull statistics	β	0.819	0.767	0.271	0.408	2.465	0.407
	θ	2.56e5	9.66e6	7.65e8	6.34e6	9.60e4	4.82e6
	R^2	82.1%	95.8%	80.0%	89.0%	83.3%	87.9%

Table 3. Statistics for SnPb Solder with Sn/Ni Pin Plating

SnPb Solder with Sn/Ni Pins							
Board Type		ImAg			ENIG		
%Ni Contamination		0.01	0.02	0.05	0.01	0.02	0.05
Population statistics	# failed	1	1	3	0	0	4
	# did not fail	21	23	20	24	24	20
	# samples	22	24	23	24	24	24
Failure statistics	rate	4.5%	4.2%	13.0%	0.0%	0.0%	16.7%
	first	6277	1198	16	n/a	n/a	1910
	average	6277	1198	772.3	n/a	n/a	3184
	median	6277	1198	304	n/a	n/a	2694
	last	6277	1198	1997	n/a	n/a	5437
Weibull statistics	β	n/a	n/a	0.291	n/a	n/a	1.43
	θ	n/a	n/a	2.51e6	n/a	n/a	1,71e4
	R^2	n/a	n/a	99.8%	n/a	n/a	79.3%

Table 4. Statistics for SAC305 Solder with Au/Ni Pin Plating

SAC305 Solder with Au/Ni Pins							
Board Type		ImAg			ENIG		
%Ni Contamination		0.05	0.07	0.1	0.05	0.72	0.1
Population statistics	# failed	8	4	17	2	9	17
	# did not fail	136	140	127	117	134	124
	# samples	144	144	144	119	143	141
Failure statistics	rate	5.6%	2.8%	11.8%	1.7%	6.3%	12.1%
	first	44	23	10	3386	6	20
	average	3289.9	2505	3552.7	3646.5	1325.1	2750.6
	median	3807	1472	2952	3646	96	1727
	last	6794	7052	7523	3907	7581	6851
Weibull statistics	β	0.465	0.288	0.438	n/a	0.293	0.618
	θ	5.23e6	2.52e9	1.65e6	n/a	3.90e7	2.31e5
	R^2	96.0%	99.9%	94.3%	n/a	83.1%	86.8%

With the limited number of failures that occurred during this test, there is insufficient data to directly compare the reliability characteristics of the different configurations that were tested. An issue of interest, however, is whether elevated nickel contamination in the solder bath increased the number of early failures resulting from assembly defects. Given the extremely low Weibull shape factors calculated for almost all the combinations shown in the preceding tables, virtually all failures observed in this testing are likely early failures (i.e., not representative of the overall failure distributions of the populations). To assess the impact of nickel contamination on these early failures, the failure data were grouped into bins of 1000 thermal cycles corresponding to the level to which they had survived. For example, a component that failed anywhere between 0 and 999 cycles was assigned to the 0-cycle bin; components that failed anywhere between 1000 and 1999 cycles were assigned to the 1000 cycle bin, etc. The number of components in each bin was normalized by the total number of samples in each population and the resulting cumulative failure distributions for each combination are shown in Figure 7. Banners on the sides of the plots show groupings for solder alloy and pin metallization. Solid lines correspond to boards with ENIG surface finish while dashed lines correspond to boards with ImAg surface finish. In each plot, blue lines indicate the lowest level of nickel contamination included in the study, red indicates the highest level of nickel contamination, and green indicates the central level of nickel contamination.

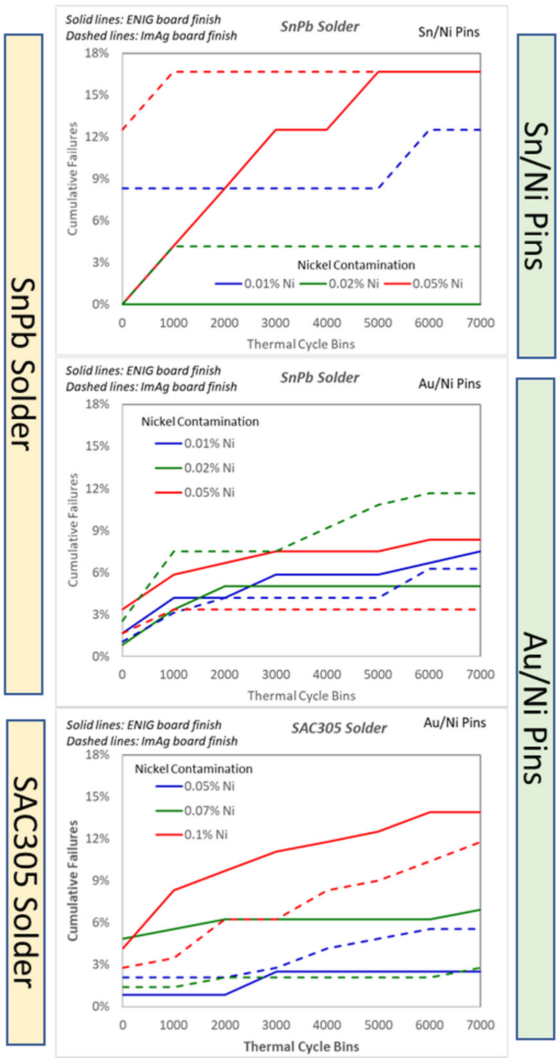

Figure 7. Comparisons of Cumulative Failures (bin size of 1000 cycles)

If the higher levels of nickel contamination used in this study substantially decreased solder joint reliability, Figure 7 would tend to have corresponding red lines (the highest level of nickel contamination) above green lines (the middle level of nickel contamination), which should then be above the blue lines (the lowest level of nickel contamination). This does occur in only one case: ENIG boards assembled with SAC305 solder.The other cases do not show a consistent trend. In the absence of such a trend, the results do not indicate that the components assembled with solder alloys with the higher nickel contamination levels in this study experienced a higher failure rate.

Close inspection of Figure 7 does indicate that the 0 cycle bin data, which lie on the y-axes of the plots, exhibit a trend of the red lines (highest nickel contamination) having higher failure rates than the blue lines (lowest nickel contamination). This indicates that the parts assembled with solder with higher nickel contamination may have a greater proportion of failures that occur before 1000 cycles than those with lower nickel contamination. Figure 8 shows the portion of solder joints that failed prior to 1000 thermal cycles for each combination of solder, pin metallization, board surface finish, and nickel contamination in the solder. One combination (SnPb, ENIG/SnNi) had no failures. For the other five combinations, the parts assembled with the solder with the highest nickel contamination (red) consistently exhibited more failures than those assembled with the solder with the lowest nickel contamination. However, this trend is not monotonic. In each of the five cases with failures prior to 1000 cycles, the medium level of contamination had either fewer failures than the lowest contamination or more failures than the highest contamination.

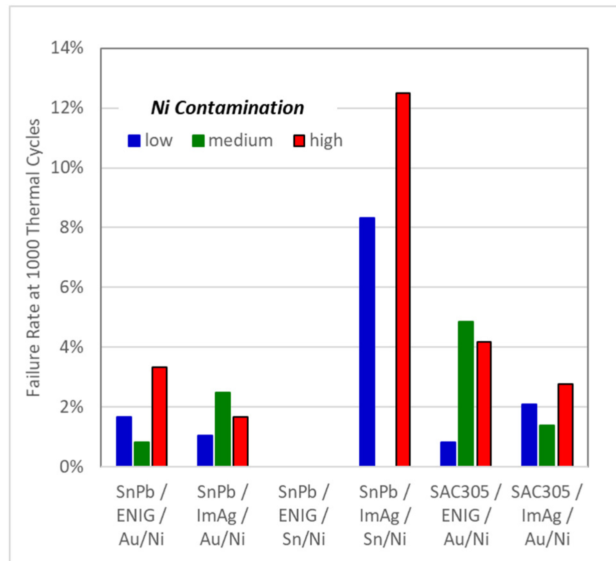

Figure 8. Impact of Nickel Contamination on Failures Occurring before 1000 Thermal Cycles

Failure Analysis

Metallographic cross-sectional analysis was conducted on the plated through holes to physically validate the event detector continuity measurements, to assess the solder joint quality characteristics of wetting/plated through hole fill, and to evaluate the solder joint microstructure/intermetallic phases. Metallographic cross-sectioning of plated through hole (PTH) components is more complex than the cross-sectioning of SMT type components due to solder joint geometry. The tangency of the cross-sectional plane in relation to the 360° plated through hole geometry and/or the angle of the lead in the solder joint prompted the extra validation efforts.

Metallographic Cross-section Results

Reviewing the SnPb and SAC305 solder joints metallurgical cross-sections produced the following observations:

• The X-ray assessment included additional cross-sectioning, with results compared to the event detector data. These assessments validated that the event detection measurements correctly identified solder joints as being failed or non-failed.

• The majority of the SnPb cross-sections showed solder joint damage due the global Coefficient of Thermal Expansion

(CTE) mismatch stresses induced by the thermal cycling. Grain coarsening was evident in the SnPb solder joint microstructures. In comparison, the SAC305 cross-sections had significantly less solder joint cracking, which exhibited typical "spider web" characteristics with some solder joint microstructure coarsening in the crack path. Coarsening of the Ag3Sn intermetallic compound (IMC) phase in the SAC305 solder joint microstructure is also evident. At the end of thermal cycle testing, all solder joints were observed to have some amount of cracking. While there was evidence of shrinkage voids in the SAC305 solder joints, industry data have shown that shrinkage voids play no role in the degradation of solder joint integrity [18].

• Some component insertion damage to the plated through hole knee was observed for both the SnPb and SAC305 solder joints. The authors believe that the knee damage was not sufficient to influence the thermal cycle results. No cracking of the plated through hole copper walls or internal layer interfaces was observed.

Figure 9 - Figure 12 show representative cross sections of components with different solder and surface finish combinations. Additional cross sections showing results for other levels of nickel contamination are shown in Appendix A.

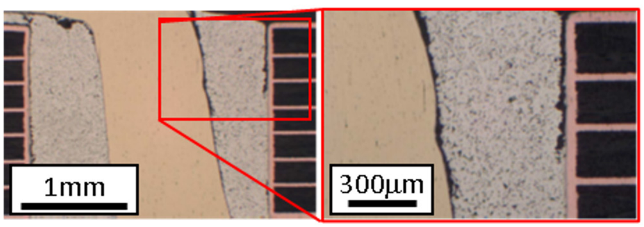

Figure 9. SnPb Solder, ENIG Surface Finish with Au/Ni Pin Finish, 0.01% Ni Contamination, Failed at 7330 Cycles

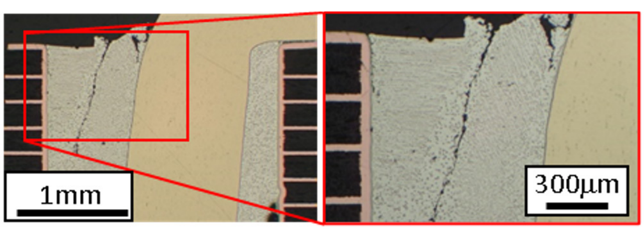

Figure 10. SAC305 Solder, ENIG Surface Finish with Au/Ni Pin Finish, 0.05% Ni Contamination, Failed at 3386 Cycles

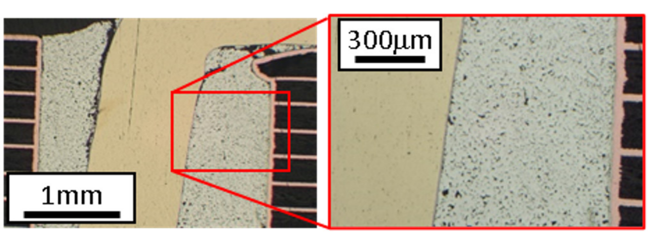

Figure 11. SnPb Solder, ImAg Surface Finish with Au/Ni Pin Finish, 0.01% Ni Contamination, Did Not Fail

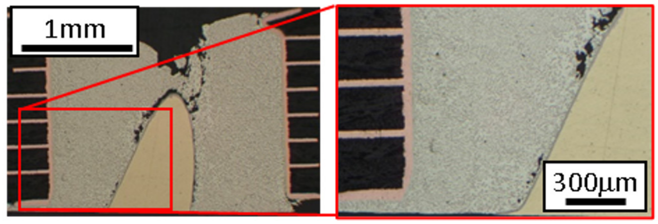

Figure 12. SAC305 Solder, ImAg Surface Finish with Au/Ni Pin Finish, 0.05% Ni Contamination, Failed at 6794 Cycles

Solder Pot Contamination Analysis

The MacDermid Alpha Electronic Solutions Analytical Laboratory conducted nickel contamination level testing on the initial solder billets. Additionally, a solder pot sample was collected after each test vehicle assembly with that solder was completed. Inductively coupled plasma mass spectroscopy (ICP) analysis was used to measure the nickel contamination levels. The initial solder pot nickel contamination levels selected as part of the investigation parameters are shown in Table 5. The amount of nickel that accumulated in the solder pot, as contributed by the test vehicle ENIG surface finish and the shorting jumper components, is reflected in the "after processing" column. The ICP measurements illustrate the affinity of the solder pot for increasing nickel contamination when many assemblies are processed. Unlike some elemental contaminants that will accumulate in the solder pot dross and are then removed during de-drossing operations, nickel slowly builds up in the solder pot, leading to an "exceeds process control limit" condition.

Table 5. Inductively Coupled Plasma Mass Spectroscopy Solder Pot Nickel Contamination Measurements

Solder alloy	Initial Nickel Contamination Level (wt.%)	Nickel Level After Processing Test Vehicles (wt.%)
SnPb	0.010	0.0230
SnPb	0.020	0.0250
SnPb	0.050	0.0403
SAC305	0.050	0.0465
SAC305	0.070	0.1018
SAC305	0.100	0.0605

Scanning Electron Microscopy (SEM) Element Mapping

SEM elemental mapping analysis, using a Hitachi SU3500 system was conducted on a series of metallographic cross-section samples to determine the distribution of nickel in the SnPb and SAC305 solder joints. The SEM mapping was conducted after thermal cycle testing was completed in order to assess whether any segregation or intermetallic compound (IMC) nickel-containing phase coalescence occurred as the result of solder joint stress. The SEM elemental maps reveal uniform nickel distribution within the solder joints for both solder alloys and their respective nickel contamination limits. Nickel plating from the ENIG board and the shorting jumper component finish is visible in the SEM element maps. No regions of nickel segregation were observed. Figure 9 -Figure 12 are SEM element mapping images illustrating the typical element distributions for the combinations of solder alloy/nickel contamination levels used in the investigation. Additional SEM results are shown for other test combinations in Appendix B.

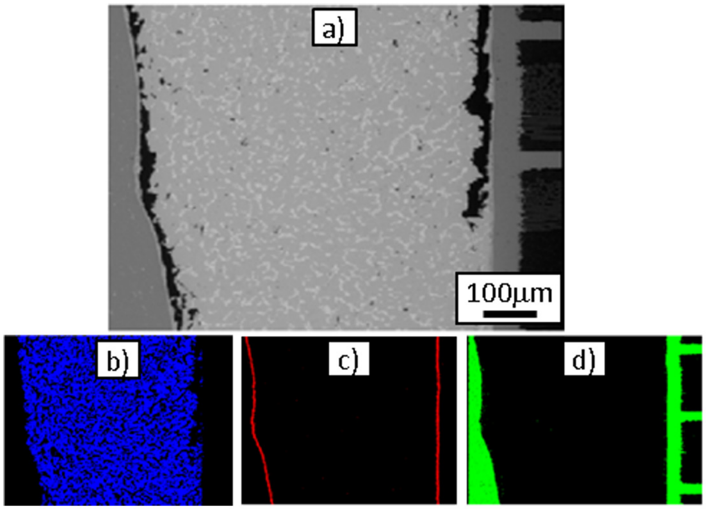

Figure 13. SEM Nickel Element Distribution Map for SnPb/0.01% Nickel Contamination: a) SEM view, b) Tin Map, c) Nickel Map, d) Copper Map

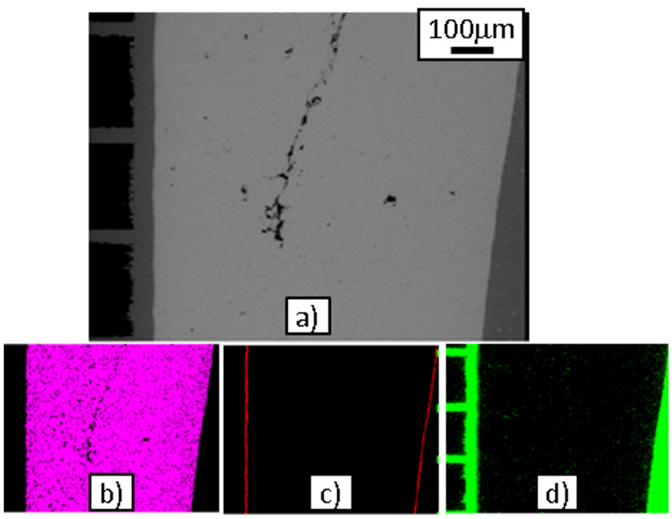

Figure 14. SEM Nickel Element Distribution Map for SAC305/0.05% Nickel Contamination: a) SEM view, b) Tin Map, c) Nickel Map, d) Copper Map

Tin Whisker Inspection Results

A portion of the test vehicles utilized Mill-Max shorting jumpers with a tin/nickel plating finish that provided the opportunity for tin whiskers to occur. Tin whiskers are crystallographic structures that are associated with stressed tin plating. The test vehicles that contained shorting jumpers with the tin/nickel plating finish were optically inspected using multiple angle light sources and a 1X-120X magnification range. No instances of tin whiskers were observed on any of the shorting jumpers.

DISCUSSION

Extended thermal cycle testing of shorting pins in through hole vias led to a relatively small number of failures. By the end of testing (7,581 thermal cycles) each of the test combinations exhibited 80-100% survival. Therefore, there were insufficient data for statistical analysis to accurately characterize the life of the test populations. The results do indicate that the failures that did occur were likely early failures that were not representative of the test populations.

Of the six test combinations (solder /board surface finish / pin metallization) included in the study, only one (SAC305 solder, ENIG board surface finish, and AuNi pin metallization) showed a trend of higher thermal cycle failure rates when the solder had more nickel contamination. The other five combinations did not exhibit any strong trends to indicate that increased nickel contamination affected the failure rate.

When limiting the analysis to failures that occurred within the first 1000 thermal cycles, 5 of the 6 test combinations did exhibit relatively more early failures in those components that were assembled with the highest level of solder pot nickel contamination. However, these differences were not significant and the trend was not consistent. In 3 of these 5 cases, the middle level of nickel contamination had the lowest early failure rate, but in the other 2 cases, those solder joints with solder with the middle level of contamination had the highest failure rates. Thus, the results do not reveal any statistically consistent or significant trends indicating that the level of nickel contamination in the solder pot, within the ranges assessed in this study, affects either the overall reliability of the solder joints or the occurrence of early failures.

During the course of the investigation, the results of a nickel contamination limit study by Robert Bosch automotive electronics group [19] were released. The Bosch investigation tested nickel contamination of SAC305 plated through hole solder joints up to a maximum 0.0625 nickel weight percent with thermal cycle conditioning (

Figure 15) using three different mechanical loads. The differences between the current study and the Bosch study, which are listed below, provide insight into the role of nickel contamination on solder joint integrity:

• The Bosch study only completed a maximum of 1000 thermal cycles (TW) while the current investigation completed almost 7000 thermal cycles.

• The Bosch study had a mechanical load parameter in their test to simulate a connector type PTH application. The current investigation closely mimicked a PTH component application with the test articles.

• The Bosch study found cracking in the PTH copper plating whereas the current investigation observed no copper plating cracks

• The Bosch study only investigated SAC305 solder with a nickel contamination range of 0 wt. % to 0.0625 wt. %; the current investigation tested both SnPb and SAC305 solders and used higher nickel contamination levels

A primary conclusion from the Bosch study was that normal solder joint crack propagation behavior had statistically greater influence on plated through hole damage than the level of nickel contamination. The results of this investigation lead to the same conclusion, despite the parameter differences. The Bosch study lends additional confidence on proposing an increase in the nickel contamination limits in the IPC-J-STD-001 specification.

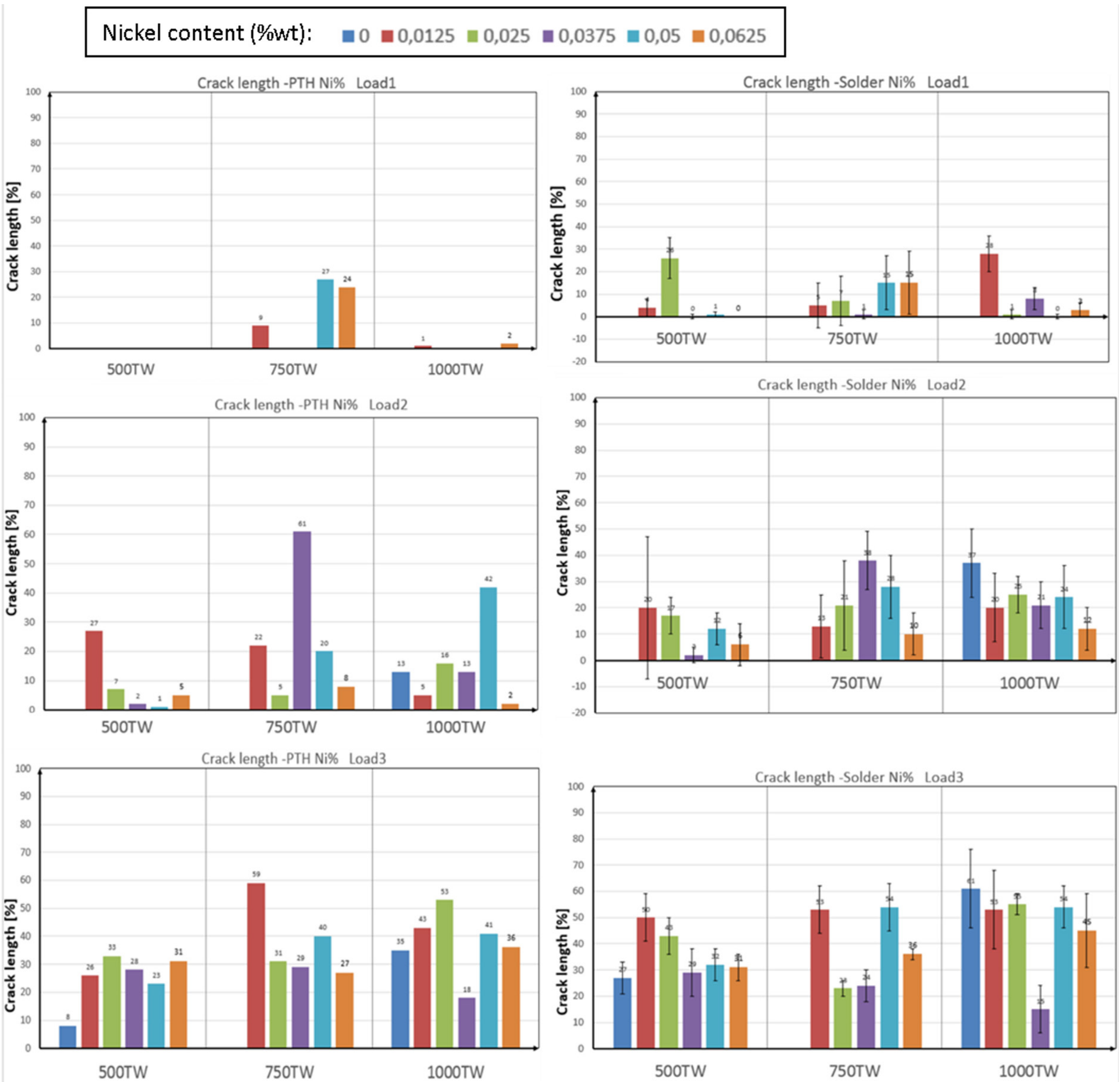

Figure 15. Robert Bosch Automotive Electronics Nickel Contamination Crack Propagation Length Versus Thermal Cycles Test Results for Copper Plating Cracks (left) and Solder Cracks (right) [19]

Increasing the allowable nickel content in selective solder and wave solder pots could potentially improve overall plated through hole solder joint integrity. Diepstraten [13], Sweatman [20, 21] and Anderson [21] published results showing that the solder nickel content has a direct positive effect on solder alloy characteristics by influencing the wetting/fluidity, solder joint microstructure refinement and stabilization of intermetallic compound (IMC) phases in both SnPb and Pb-free solder alloys. Figure 16 illustrates the influence of solder alloy nickel content on the interfacial IMC cracking behavior.

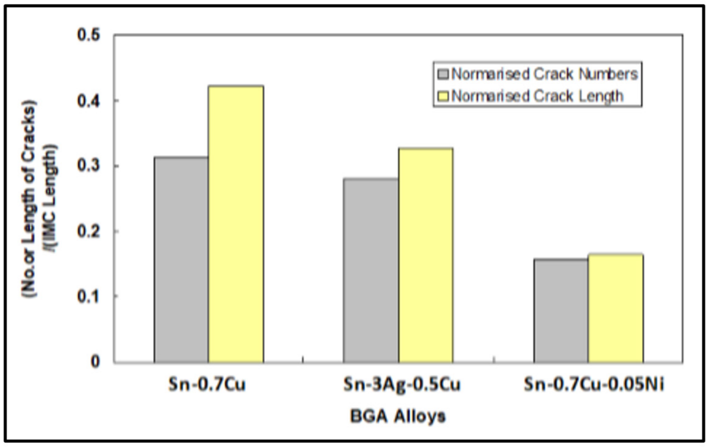

Figure 16. Sweatman Data Illustrating Interfacial IMC Cracking Behavior as a Function of Solder Alloy Nickel Content [21]

It should be noted that the IPC-J-STD-001 specification Table 3-1, Maximum Limits of Solder Bath Contaminant, also contains SnPb solder alloy maximum contamination limits for solder pots used for Preconditioning activities. The Preconditioning SnPb solder alloy maximum nickel contamination limit is 0.025 wt.%. Preconditioning SnPb solder alloy maximum contamination limits for different elements are greater than, or equal to, the maximum contamination limits used for the Assembly soldering maximum contamination limits. Based on the investigation results, the Preconditioning SnPb solder alloy maximum nickel contamination limit should be equal to the Assembly soldering maximum nickel contamination limit.

CONCLUSION

The investigation produced insufficient data to accurately characterize the life of any of the test populations, even after completing 7,581 thermal cycles. Physical failure assessment, using metallographic cross-sectioning and SEM elemental mapping analyses, found no correlation between nickel contamination levels and plated through hole solder joint integrity for either the SnPb or SAC305 solder alloys. The authors recommend that the allowable nickel contamination levels listed in the IPC-J-STD-001 specification Table 3-1, Maximum Limits of Solder Bath Contaminant, be modified to 0.05 wt.% for SnPb Assembly, 0.05 wt.% for SnPb Preconditioning and 0.10 wt.% for SAC305 Pb-free Assembly.

ACKNOWLEDGMENTS

The authors would like to thank Ken Blazek, Grace Cooke, Kristin Sheyko, Alex Faucz for thermal cycle testing and metallographic cross-section processing, Dwayne Koch for SEM elemental mapping analysis and MacDermid Alpha Electronic Solutions Analytical Laboratory for solder alloy preparation/analysis efforts.

REFERENCES

1. M. Heberlein, "Effect of Impurities on Some Properties of Lead-Tin Alloys," in Papers on Soldering (1962), edited by Committee B-2 (West Conshohocken, PA: ASTM International, 1963), 29-38.
2. M.L. Ackroyd, C.A. MacKay, C.J. Thwaites, Effect of Certain Impurity Elements on the Wetting Properties of 60% Tin – 40% Lead Solders, International Tin Research Institute, Publication 493, 1975.
3. C.A. MacKay, “Causes and Effects of Solder Contamination: Part I, Electronics, March 1983.
4. C.A. MacKay, “Causes and Effects of Solder Contamination: Part II, Electronics, April 1983.
5. C.A. MacKay, “Causes and Effects of Solder Contamination: Part III, Electronics, May 1983.
6. H. Steen and G. Becker, “The Effect of Impurity Elements on the Soldering Properties of Eutectic and Near-eutectic Tin-lead Solder”, Brazing & Soldering, No. 11, Autumn 1986.
7. D. Bernier, “The Effect of Metallic Impurities on the Wetting Properties of Solder”, Kester Solder Technical Article, 1994, pg. 1.
8. D. Hillman et al., “Dissolution Rate of Electronics Packaging Surface Finish Elements in Sn3.0Ag0.5Cu Solder”, Journal of Electronic Materials, August 2019, Volume 48, Issue 8.
9. C.M.L. Wu and Y.W. Wong, “Rare Earth Additions to Lead-free Electronic Solders”, Lead-free Electronic Solders, ISBN 0-387-48431-0, Springer Science Business Media LLC, 2007.
10. R. Coyle et al., “The Effect of Bismuth, Antimony, or Indium on the Thermal Fatigue of High Reliability Pb-Free Solder Alloys”, SMTAI Conference proceedings, Chicago, 2018, pg. 15.
11. A. Gickler et al., “Contamination of Lead Free Solders with Copper and Lead”, SMTA TechScan Compendium: The State of the Art in Pbfree Soldering Technology, SMTA, 2003.
12. A. Forsten et al., “Development and Validation of Lead-free Wave Soldering Process”, Soldering & Surface Mount Technology, Vol. 12, No.3, 2000.
13. G. Diepstraten and H. Trip, “How to Manage Wave Solder Alloy Contaminations”, IPC Midwest Conference proceedings, 2007, pg. 17-20.
14. K. Nogita et al., “The Role of Nickel in Solder Alloys – Part I: The Effect of Ni on the Behavior of Sn-0.7Cu in Soldering and Coating Process”, SMTAI Conference proceedings, Chicago, 2018.
15. K. Nogita et al., “The Role of Nickel in Solder Alloys – Part II: The Effect of Ni on the Integrity of the Interfacial Intermetallic in S Based/Cu Substrate on Solder Joints”, SMTAI Conference proceedings, Chicago, 2018.
16. M. Ramli et al., “The Effect of Ni and Bi Additions on the Solderability of Sn -0.7Cu Solder Coatings”, Journal of Electronic Materials, January 2020, Volume 49, Issue 1.

17. IPC Solder Products Value Council Report, SPVC-TAL1, November 2009.

18. M. Ribas, et al, "Effect of Voids on Thermo-Mechanical Reliability of Solder Joints", SMTAI Conference proceedings, Chicago, 2017, pg. 6.

19. U. Welzel, Robert Bosch Automotive Electronics group Technical Data.

20. K. Sweatman, T. Nishimura, K. Nogita, "The Role of Nickel in Solder Alloys – Part 1. The Effect of Ni on the Behaviour of Sn-0.7Cu In Soldering and Coating Processes", SMTAI Conference Proceedings, October 2018, pg. 2.

21. K. Sweatman, T. Nishimura, K. Nogita, "The Role of Nickel in Solder Alloys – Part 2. The Effect of Ni on the Integrity of The Interfacial Intermetallics in Sn-Based/Cu Substrate Solder Joints", SMTAI Conference Proceedings, October, 2018, pg. 6.

22. I. Anderson, S. Choquette, "Intermetallic Formation of Sn Solder on Cu-XNi for a Harsh Environment Composite Solder Paste", SMTA Pan Pacific Microelectronics Symposium Proceedings, 2018.

APPENDIX A

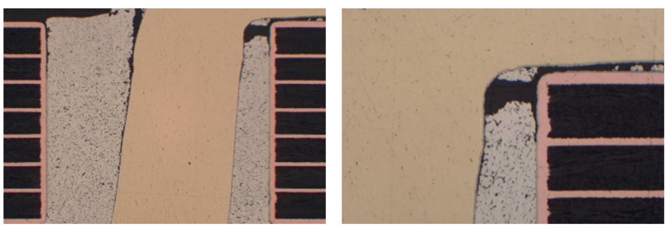

Figure 17. SnPb Solder, ENIG Surface Finish with Au/Ni Pin Finish, 0.01% Ni Contamination, Did Not Fail

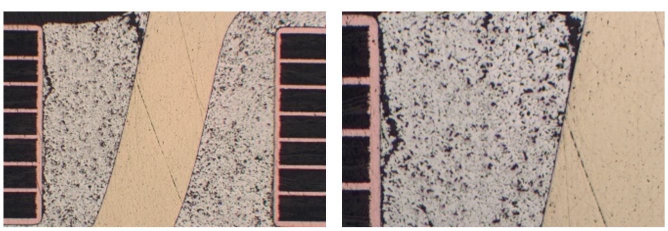

Figure 18. SnPb Solder, ENIG Surface Finish with Au/Ni Pin Finish, 0.02% Ni Contamination, Failed at 2753 Cycles

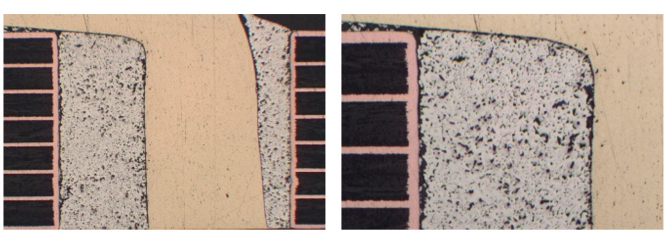

Figure 19. SnPb Solder, ENIG Surface Finish with Au/Ni Pin Finish, 0.02% Ni Contamination, Did Not Fail

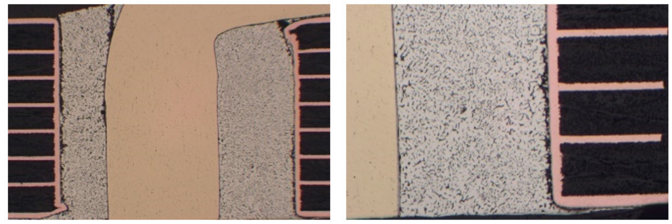

Figure 20. SnPb Solder, ENIG Surface Finish with Au/Ni Pin Finish, 0.05% Ni Contamination, Failed at 6589 Cycles

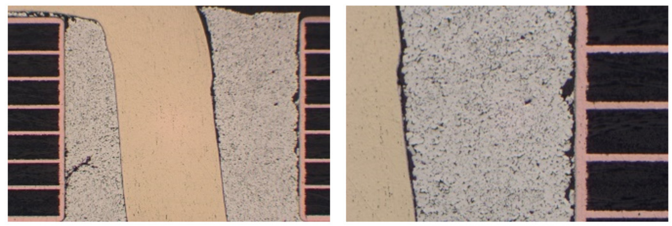

Figure 21. SnPb Solder, ENIG Surface Finish with Au/Ni Pin Finish, 0.05% Ni Contamination, Did Not Fail

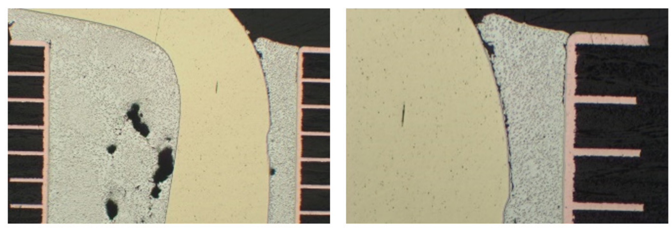

Figure 22. SAC305 Solder, ENIG Surface Finish with Au/Ni Pin Finish, 0.05% Ni Contamination, Did Not Fail

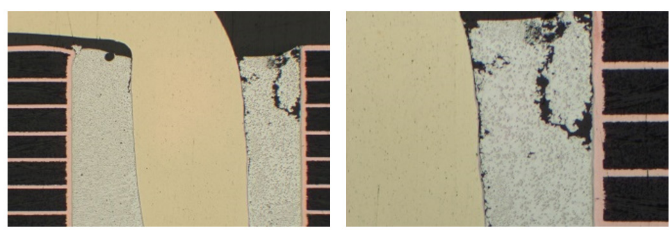

Figure 23. SAC305 Solder, ENIG Surface Finish with Au/Ni Pin Finish, 0.07% Ni Contamination, Failed at 2078 Cycles

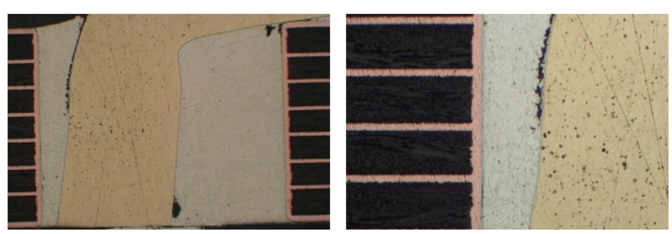

Figure 24. SAC305 Solder, ENIG Surface Finish with Au/Ni Pin Finish, 0.07% Ni Contamination, Did Not Fail

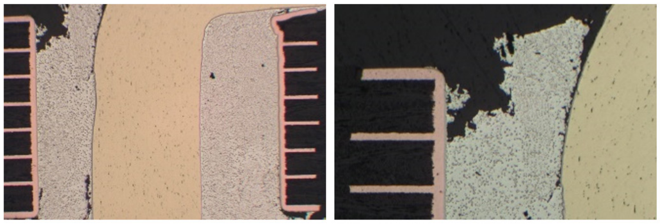

Figure 25. SAC305 Solder, ENIG Surface Finish with Au/Ni Pin Finish, 0.1% Ni Contamination, Failed at 6851 Cycles

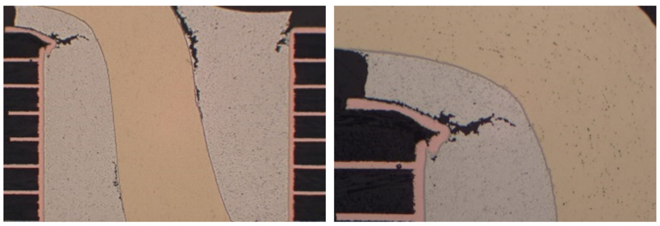

Figure 26. SAC305 Solder, ENIG Surface Finish with Au/Ni Pin Finish, 0.1% Ni Contamination, Did Not Fail

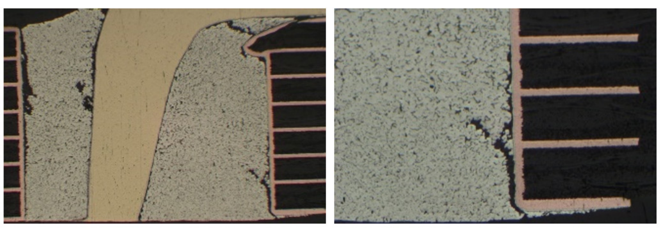

Figure 27. SnPb Solder, ImAg Surface Finish with Au/Ni Pin Finish, 0.01% Ni Contamination, Failed at 6077 Cycles

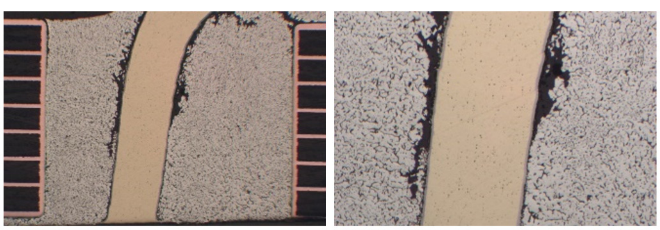

Figure 28. SnPb Solder, ImAg Surface Finish with Au/Ni Pin Finish, 0.02% Ni Contamination, Failed at 2064 Cycles

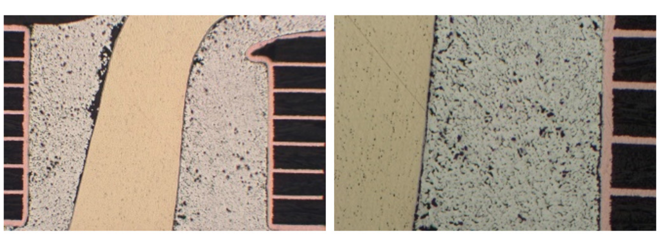

Figure 29. SnPb Solder, ImAg Surface Finish with Au/Ni Pin Finish, 0.02% Ni Contamination, Did Not Fail

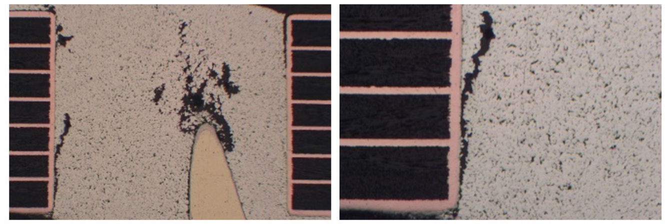

Figure 30. SnPb Solder, ImAg Surface Finish with Au/Ni Pin Finish, 0.05% Ni Contamination, Failed at 1112 Cycles

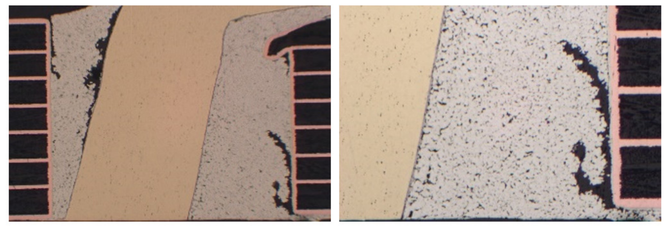

Figure 31. SnPb Solder, ImAg Surface Finish with Au/Ni Pin Finish, 0.05% Ni Contamination, Did Not Fail

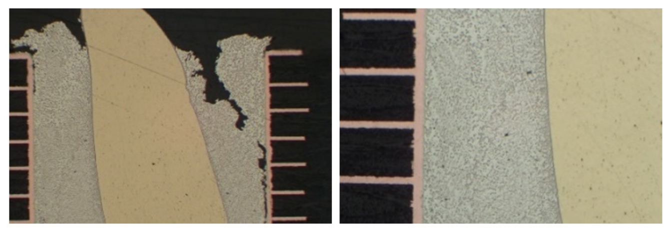

Figure 32. SAC305 Solder, ImAg Surface Finish with Au/Ni Pin Finish, 0.05% Ni Contamination, Did Not Fail

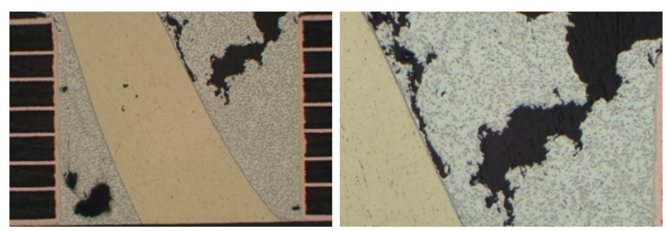

Figure 33. SAC305 Solder, ImAg Surface Finish with Au/Ni Pin Finish, 0.07% Ni Contamination, Failed at 7052 Cycles

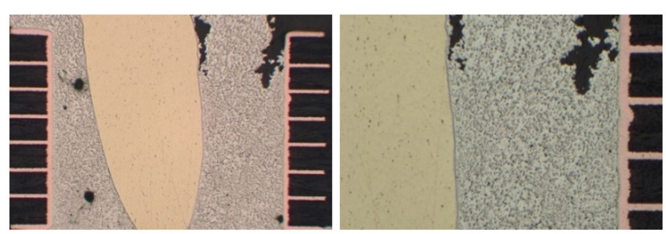

Figure 34. SAC305 Solder, ImAg Surface Finish with Au/Ni Pin Finish, 0.07% Ni Contamination, Did Not Fail

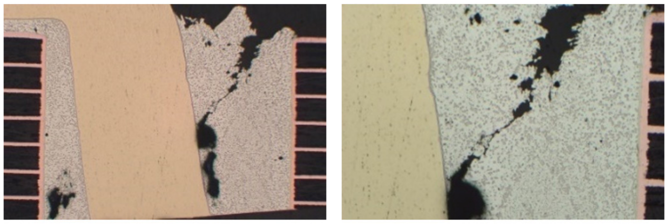

Figure 35. SAC305 Solder, ImAg Surface Finish with Au/Ni Pin Finish, 0.1% Ni Contamination, Failed at 7523 Cycles

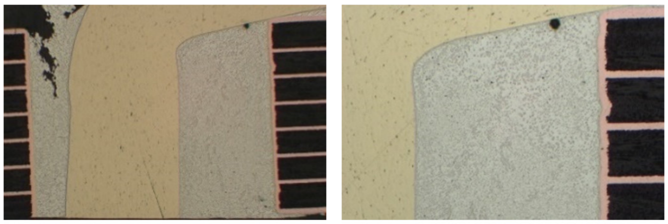

Figure 36. SAC305 Solder, ImAg Surface Finish with Au/Ni Pin Finish, 0.1% Ni Contamination, Did Not Fail

APPENDIX B

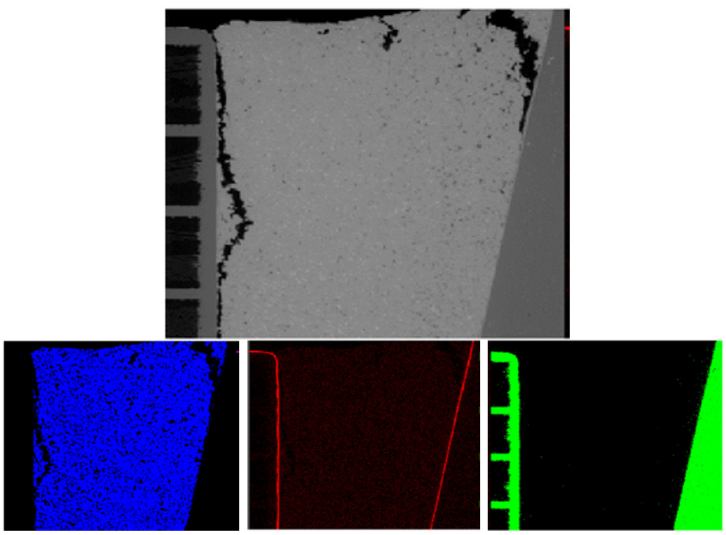

Figure 37. SEM Nickel Element Distribution Map for SnPb/0.02% Nickel Contamination: SEM view (top), Tin Map (left), Nickel Map (center), Copper Map (right)

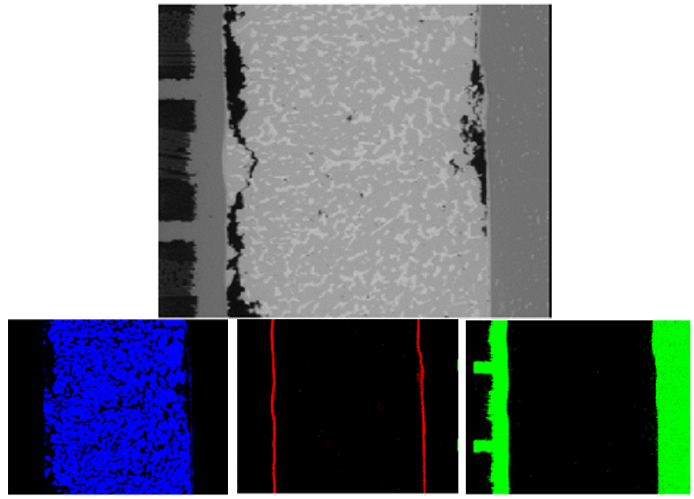

Figure 38. SEM Nickel Element Distribution Map for SnPb/0.05% Nickel Contamination: SEM view (top), Tin Map (left), Nickel Map (center), Copper Map (right)

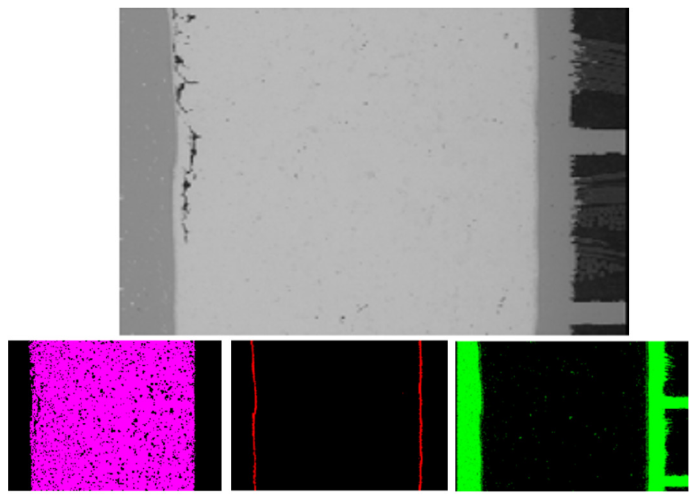

Figure 39. SEM Nickel Element Distribution Map for SAC305/0.07% Nickel Contamination: SEM view (top), Tin Map (left), Nickel Map (center), Copper Map (right)

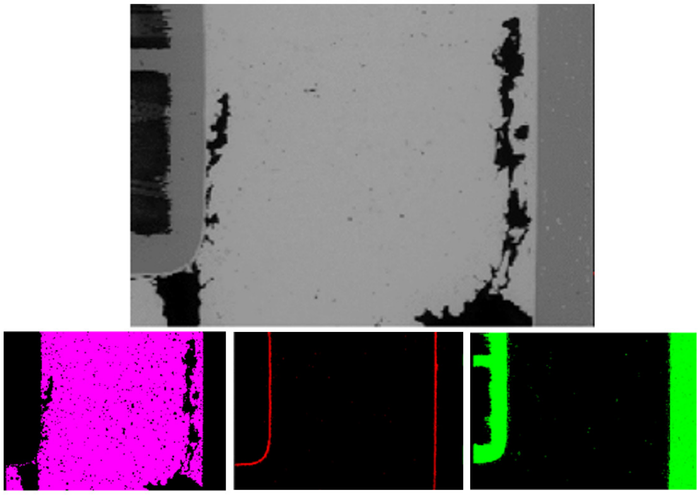

Figure 40. SEM Nickel Element Distribution Map for SAC305/0.10% Nickel Contamination: SEM view (top), Tin Map (left), Nickel Map (center), Copper Map (right)

BIOGRAPHIES

David D. Hillman is a Metallurgical Engineer in the Advanced Operations Engineering Department of Rockwell Collins Inc. in Cedar Rapids, Iowa. Mr. Hillman graduated from Iowa State University with a B.S. (1984) and M.S. (2001) in Material Science & Engineering. In his present assignment he serves as a consultant to manufacturing on material and processing problems. He served as a Subject Matter Expert (SME) for the Lead-free Manhattan Project in 2009. He has published 200+ technical papers. Mr. Hillman was named a Rockwell Collins Fellow in 2016. He was named an IPC Raymond E. Prichard Hall of Fame award recipient in 2018. He serves as the Chairman of the IPC JSTD-002 Solderability committee. Mr. Hillman served as a Metallurgical Engineer at the Convair Division of General Dynamics with responsibility in material testing and failure analysis prior to joining Rockwell. He is a member of the American Society for Metals (ASM), the Minerals, Metals & Materials Society (TMS), and Surface Mount Technology Association (SMTA) and the Institute for Interconnecting and Packaging of Electronic Circuits (IPC).

Ross Wilcoxon is an Engineering Fellow with Collins Aerospace in Cedar Rapids, Iowa, USA. He conducts research and supports product development of thermal management, reliability and electronics packaging technologies for avionics systems. He is an editor of Electronics Cooling Magazine and received the SEMI-THERM Symposium Thermi Award in 2021. Prior to joining Collins in 1998, he was an assistant professor of mechanical engineering at South Dakota State University.

Denis Jean is a Process Specialist with Kurtz Ersa providing technology support for soldering application. He has over 35 years of experience of supporting both domestic and foreign OEM's and EMS companies in product design, soldering material development, process and assembly/rework equipment development for surface mount and through-hole soldered assemblies. Denis has authored, instructed and presented frequently on topics including through hole soldering (wave/selective), SMT assembly, DFM/DFX and rework. He has received 2 patents for his work with polymer thick film technology. He was serving on the SMTA-I technical committee for several years.